Pharmaceutical Sciences and Drug Design
ISSN: 3062-4428
2025, Volume 5, Page No: 96-113

Available online at: www.galaxypub.co/page/journals

Galaxy Publication

Hippocampal Angiogenesis Driven by the SIRT1/FOXO1 Pathway Contributes to the Antidepressant Actions of Chaihu Shugan San

Olivia Turner[1]*, Hazel Grant[1], Mia Douglas[1]

[1]Department of Biotechnology, Faculty of Science, University of Auckland, Auckland, New Zealand.

***E-mail** ✉ olivia.turner.nz@outlook.com
Received: 01 March 2025; **Revised:** 28 May 2025; **Accepted:** 02 June 2025

ABSTRACT

Chaihu Shugan San (CSS), a classical formula long employed in the management of major depressive disorder (MDD), has repeatedly demonstrated both efficacy and safety in clinical settings. Impaired angiogenesis has emerged as a critical component of MDD pathology, yet the specific mechanisms by which CSS influences angiogenic processes remain insufficiently defined. To clarify these mechanisms, network pharmacology was first used to map potential angiogenesis-related targets and pathways linking CSS and MDD. Candidate targets were subsequently examined in a chronic unpredictable mild stress (CUMS) mouse model using Western blotting, immunofluorescence, and immunohistochemistry. Mechanistic exploration continued in brain microvascular endothelial cells (BMVECs) treated with CSS-containing serum, assessed through Western blotting and immunofluorescence. Computational analysis highlighted the Silent information regulator protein 1 (SIRT1)/Forkhead box O1 (FOXO1) axis as a central mediator of CSS-associated angiogenesis, a prediction validated experimentally. In CUMS mice, CSS enhanced angiogenic activity, elevated SIRT1, and reduced FOXO1 within the hippocampus. Treatment of BMVECs with 5% CSS-containing serum markedly stimulated cell proliferation, migration, and tube-forming capacity; however, these pro-angiogenic responses diminished when SIRT1 was silenced. CSS-conditioned serum also promoted FOXO1 cytoplasmic translocation via SIRT1 signaling, facilitating FOXO1 degradation. In addition, CSS elevated VEGFA and BDNF levels both in hippocampal tissue from depressive mice and in BMVECs supernatants, two trophic factors central to neurogenesis. CSS supports both angiogenesis and neurogenesis in the hippocampus of CUMS-exposed mice, largely through modulation of the SIRT1/FOXO1 pathway and downstream enhancement of VEGFA and BDNF. These results suggest new avenues for CSS-based therapeutic development and indicate that targeting the SIRT1/FOXO1 axis may hold promise for future MDD treatment strategies.

Keywords: Major depressive disorder, Brain microvascular endothelial cell, Chaihu Shugan San, Angiogenesis, SIRT1/FOXO1 axis

How to Cite This Article: Turner O, Grant H, Douglas M. Hippocampal Angiogenesis Driven by the SIRT1/FOXO1 Pathway Contributes to the Antidepressant Actions of Chaihu Shugan San. Pharm Sci Drug Des. 2025;5:96-113. https://doi.org/10.51847/CV0RYDBQVQ

Introduction

Major depressive disorder (MDD) is a complex psychiatric condition marked by high prevalence, heterogeneous symptom profiles, multifactorial etiologies, and still-uncertain biological underpinnings [1]. In clinical practice, conventional antidepressants fail to provide adequate benefit for a substantial proportion of patients; only about 40–60% demonstrate a therapeutic response, roughly one-third attain full remission, and nearly 30% develop treatment resistance even when managed according to established guidelines [2]. In addition, these agents frequently provoke adverse reactions such as gastrointestinal discomfort, visual disturbances, and sexual dysfunction [3, 4]. Although ketamine produces a rapid and noteworthy antidepressant response, its clinical usefulness is constrained by psychotomimetic effects and potential for misuse [5, 6]. Other therapeutic modalities, including psychotherapy and repetitive transcranial magnetic stimulation (rTMS), offer certain benefits but also present notable limitations—rTMS often induces scalp pain during stimulation (~40%) and transient headaches afterward (~30%) [7], whereas psychotherapy, though minimally invasive, is mainly recommended for mild

depression [8]. Consequently, the search for novel antidepressant treatments with enhanced efficacy and fewer undesirable effects has become a key research priority.

Chaihu Shugan San (CSS), a long-standing traditional Chinese medicine (TCM) prescription, is widely applied in China for depression management. Meta-analyses have shown that CSS can alleviate depressive symptoms effectively and safely in MDD patients [9–11]. In one study, CSS produced a more pronounced reduction in Hamilton Depression Rating Scale (HDRS) scores than standard antidepressants and yielded a slightly higher effective rate (65.1% vs. 58.2%) [9]. Importantly, CSS has been associated with fewer adverse events, including reduced appetite, increased appetite, dry mouth, anxiety, and constipation [10, 11]. Growing experimental evidence is elucidating the biological actions of CSS: it has been shown to enhance adult neurogenesis and elevate brain-derived neurotrophic factor (BDNF) expression in rodent models displaying depression-like behaviors [12, 13]. Since brain microvessels supply essential nutrients required for neuronal development, survival, and maturation, their involvement is noteworthy. Furthermore, CSS has demonstrated anti-atherosclerotic properties and improved depressive behaviors in mice with coronary heart disease, potentially through BDNF upregulation in endothelial cells [14]. A clinical investigation also reported that CSS increased regional cerebral blood flow and reduced depressive symptoms to a degree comparable to Fluoxetine [15]. These findings collectively imply a connection between CSS and brain microvascular function; however, its direct effects on cerebral microvessels and the molecular pathways involved remain insufficiently defined.

Angiogenesis has emerged as a relevant factor in depression. Several investigations have documented reduced vascular density in the brains of depressed individuals [16–18]. Key pro-angiogenic mediators such as vascular endothelial growth factor (VEGF) and BDNF are diminished both in depressed patients and in stress-exposed animal models [19–21]. Additionally, inhibition of VEGF signaling (via SU1498) abolishes the pro-angiogenic benefits of exercise, a non-pharmacological intervention, in stressed mice [22]. These observations together support the hypothesis that angiogenic changes may participate in depression pathophysiology, though further mechanistic clarification is needed.

Silent information regulator protein 1 (SIRT1), a nicotinamide adenine dinucleotide-dependent deacetylase, is highly expressed in vascular endothelial cells [23]. Through deacetylation and subsequent regulation of downstream Forkhead box O1 (FOXO1), SIRT1 exerts substantial influence over angiogenic processes. For instance, resveratrol, a known SIRT1 activator, enhances wound repair by promoting SIRT1-driven angiogenesis and suppressing FOXO1 expression [24]. Beyond its vascular functions, SIRT1 has been implicated in depression: a recent genome-wide association study involving Han Chinese participants identified two SIRT1-related loci associated with depressive disorders [25]. Yet, the specific contributions of SIRT1 to hippocampal angiogenesis in the context of depression remain poorly defined.

In this study, chronic unpredictable mild stress (CUMS) mouse models, network pharmacology analysis, and brain microvascular endothelial cell (BMVEC) experiments were integrated to elucidate how CSS may regulate hippocampal angiogenesis in MDD. Our goal was to provide mechanistic support for considering CSS as a candidate therapeutic strategy for managing MDD.

Materials and Methods

Network pharmacology analysis

To identify the chemical constituents of Chaihu Shugan San (CSS), compounds were retrieved from the Traditional Chinese Medicine System Pharmacology Database and Analysis Platform (TCMSP; http://tcmspnw.com/, updated May 31, 2014) by searching for the individual herbs composing the formula (for example: Bupleurum falcatum L./chai hu/柴胡). Following TCMSP recommendations, compounds meeting the criteria of oral bioavailability ≥30% and drug-likeness ≥0.18 were retained as bioactive candidates, yielding a total of 116 components. These selected molecules were then converted to canonical SMILES formats using the PubChem database (https://pubchem.ncbi.nlm.nih.gov/). The SMILES strings were subsequently uploaded to the SwissTargetPrediction platform (http://www.swisstargetprediction.ch/, updated 2019) for target forecasting, restricting species to “Homo sapiens” and retaining predictions with a probability >0.

Potential therapeutic targets associated with major depressive disorder (MDD) were collected from three human protein–related databases: the Therapeutic Target Database (https://db.idrblab.org/ttd/, updated June 1, 2020), DisGeNET (http://www.disgenet.org/web/DisGeNET/, updated May 2020), and DrugBank (http://www.drugbank.ca/, released April 22, 2020), using the keywords “major depressive disorder,”

"depression," and "unipolar depression." Targets with "score" values at or above the mean were considered disease-relevant. The overlapping set of CSS targets and MDD-associated targets—147 in total—was selected for downstream analyses.

Functional enrichment was performed through the Database for Annotation, Visualization, and Integrated Discovery (DAVID; http://david.abcc.ncifcrf.gov/, updated October 2016), with species specified as "Homo sapiens" for Gene Ontology (GO) evaluation. Enriched terms with $p < 0.05$ were regarded as significant, and angiogenesis-related functions were highlighted for further investigation. Interactions among these angiogenesis-associated targets were extracted using the STRING database (https://string-db.org/, updated August 12, 2021), setting "Homo sapiens" as the organism and applying a minimum combined score of 0.4. Cytoscape v3.7.0 was used to visualize protein–protein interaction networks, and the NetworkAnalyzer plug-in was utilized to determine hub genes based on node degree, identifying targets with the highest connectivity.

Animals

The study used forty male C57BL/6 mice and twenty male Sprague–Dawley rats (6–8 weeks of age), obtained from Beijing Vital River Laboratory Animal Technology Company (Beijing, China). Animals were maintained under controlled temperature and humidity with unrestricted access to food and water unless otherwise specified. All procedures complied with the National Institutes of Health guidelines for laboratory animal care and were approved by the Experimental Animal Ethics Committee of Beijing Friendship Hospital (Grant No. 21–1008).

Drug preparation

CSS consists of seven traditional medicinal herbs: Bupleurum falcatum L. (Chai-hu, 18 g), Cyperus × aurantium L. (Xiang-fu, 18 g), Ligusticum chuanxiong Hort. (Chuan-xiong, 18 g), Citrus reticulata Blanco (Chen-pi, 18 g), Citrus × aurantium L. (Zhi-qiao, 18 g), Paeonia lactiflora Pall. (Bai-shao, 30 g), and Glycyrrhiza uralensis Fisch. (Gan-cao, 10 g). CSS granules were obtained from Beijing Tcmages Pharmaceutical Company (Beijing, China). Using the standard body surface area conversion ratio between humans and mice (9:1), the mouse dose (g/kg) was calculated as:

$$9 \times \text{adult daily herbal dose (130 g)} / \text{average adult weight (60 kg)} = 19.5 \text{ g herb/kg.} \quad (1)$$

Serum containing CSS was prepared following previously published procedures [26]. Rats were randomly allocated to either the control serum group or the CSS-containing serum group (n=10 per group). Based on the human-to-rat conversion ratio (6.25:1), rats in the treatment group received CSS by gavage at 13.5 g herb/kg daily for 10 days, while control rats received distilled water. Two hours after the final administration, rats were euthanized, and blood was collected. Sera were filtered through a 0.22 μm membrane and stored at −80 °C for later experiments.

Quality control of CSS and CSS-containing serum

High-performance liquid chromatography coupled with mass spectrometry (HPLC–MS) was used to assess the chemical profiles of CSS and CSS-derived serum. Standards were dissolved in methanol. CSS granules were dissolved in water (0.1 g/mL), vortexed for 30 minutes, and centrifuged at 14,000 rpm for 10 minutes. Serum samples were processed similarly. Samples were separated on an Agilent Zorbax XDX C18 column (50 mm × 2.1 mm × 3.5 μm; Santa Clara, CA, USA). Mobile phase A consisted of acetonitrile and phase B consisted of 0.1% formic acid aqueous solution. The gradient program was: 0–0.5 min, 20% B; 0.5–4 min, 20–80% B; 4–5 min, 80% B; 5–5.01 min, 80–20% B; 5.01–6 min, 20% B, with a flow rate of 0.5 mL/min and a column temperature of 30 °C. Injection volume was 1 μL.

Mass spectrometry was carried out using a Sciex API 4000 Qtrap MS system with a Turbo Ionspray interface (Applied Biosystems, Foster City, CA, USA). Analyses were conducted in both positive and negative electrospray ionization modes under multiple reaction monitoring conditions. High-purity nitrogen served as curtain gas (10 psi), ion source gas 1 (55 psi), and ion source gas 2 (55 psi). The spray voltage was ±4.5 kV and capillary temperature was set at 500 °C.

CUMS procedure and drug administration

Mice were assigned to three groups: a control (CON) group without stress or CSS, a CUMS group subjected to stress, and a CUMS+CSS group receiving both stress and CSS. The CUMS and CUMS+CSS mice were singly housed and exposed to a six-week chronic unpredictable mild stress (CUMS) protocol adapted from earlier work [27]. Each day, animals experienced one long-term stressor and one short-term stressor at random intervals. Long-term stressors included: overnight wet bedding, overnight constant illumination, 24-hour food deprivation, 24-hour water deprivation, 24-hour exposure to damp sawdust, and 24-hour 45° cage tilt. Short-term stressors consisted of a 10-minute tail pinch, 10-minute exposure to recorded mouse screams, and 2-hour restraint. No stressor was repeated on two consecutive days. Control mice were group-housed and briefly handled daily.

Throughout the stress period, CUMS+CSS mice received CSS by oral gavage at 19.5 g herb/kg daily, while the CON and CUMS groups were administered equal volumes of distilled water. For bromodeoxyuridine (BrdU) labeling, mice were given intraperitoneal injections of BrdU (50 mg/kg; No. B5002-250MG, Sigma, MO, USA) once daily for seven days prior to behavioral assessments.

Behavioral tests

To evaluate stress-induced anhedonia, the sucrose preference test was conducted following previously described procedures [28]. Mice were first accustomed to two drinking bottles placed in each cage for three consecutive days. After this habituation period, both food and water were withdrawn for 12 h. Animals then received free access for 24 h to two bottles—one containing plain water and the other holding a 2% sucrose solution. Liquid intake from each bottle was measured, and sucrose preference was determined as the percentage of sucrose consumption relative to the total fluid intake.

The tail suspension test (TST) served as an additional measure of antidepressant-like activity [29]. Each animal was suspended by the tail using adhesive tape placed approximately 1 cm from the tip, with the mouse hanging 30 cm above the surface. Immobility time during the 10-min session was recorded as an indicator of behavioral despair [30].

For the forced swim test (FST), mice were placed in a transparent cylindrical container (18.5 cm height, 14.5 cm diameter) filled with water (23–25 °C) to a depth of 12 cm, preventing the mice from touching the bottom. During the 10-min evaluation period, animals were considered immobile when displaying minimal movement and only performing actions required to stay afloat [31].

Tissue collection and preparation

Immediately after behavioral testing, mice were deeply anesthetized and perfused transcardially with saline to remove intravascular blood. Selected brain regions were embedded in optimal cutting temperature compound and frozen at –80 °C for subsequent cryosectioning [32]. Tissue blocks were sectioned at 10 μm thickness beginning from the anterior hippocampus. For unbiased sampling, eight sections per mouse were collected at intervals of 90 μm [33]. Additional hippocampal tissue was reserved for Western blot analysis.

Western blots

Proteins were extracted using radioimmunoprecipitation assay buffer, quantified via a bicinchoninic acid assay, separated by 10% SDS–polyacrylamide gel electrophoresis, and transferred to nitrocellulose membranes. After blocking with 5% skim milk, membranes were incubated overnight at 4 °C with primary antibodies against SIRT1 (1:1000, ab12193, Abcam), FOXO1 (1:500, sc-374427, Santa), acetylated FOXO1 (1:100, MBS9600633, MyBioSource), VEGFA (1:1000, ab1316, Abcam), or BDNF (1:1000, ab108319, Abcam). HRP-conjugated secondary antibodies (1:5000, ab8245 or ab8226, Abcam) were applied the following day. Protein signals were detected with a Bio-Rad imaging system and quantified using ImageJ software. GAPDH or β-ACTIN served as loading controls.

Immunofluorescence

Frozen sections were warmed for 30 min, fixed with 4% paraformaldehyde, and permeabilized using 0.2% Triton-X100. For BrdU staining, DNA denaturation was carried out with 2 N HCl at 37 °C for 1 h. After 5% donkey serum blocking, sections were incubated overnight with antibodies against GLUT1 (1:200, ab40084), NeuN (1:200, ab209898), CD34 (1:100, ab81289), or BrdU (1:200, ab6326). Appropriate fluorophore-labeled secondary antibodies (Alexa Fluor 488, Alexa Fluor 647, or Cy3; 1:400) were applied, and nuclei were counterstained with

DAPI. Images were captured using an Olympus fluorescence microscope. Quantification was performed at 10× magnification with eight fields per section and ten sections per mouse [34], using four biological replicates. Cultured BMVECs were stained following similar fixation, permeabilization, and blocking steps, then incubated with SIRT1 and FOXO1 antibodies (1:200), followed by Alexa Fluor-conjugated secondaries (1:200, ab150116).

Immunohistochemistry

Frozen sections were fixed, permeabilized, and blocked with goat serum for 1 h, then incubated overnight with antibodies targeting SIRT1 (1:100), FOXO1 (1:50), or GLUT1 (1:100). After incubation with goat-anti-mouse or goat-anti-rabbit secondary antibodies, staining was visualized using diaminobenzidine, followed by hematoxylin counterstaining.

Mouse BMVECs culture

To further examine the pro-angiogenic contribution of CSS, mouse brain microvascular endothelial cells (BMVECs) obtained from Procell (Wuhan, China) were cultured following standard procedures [35, 36]. Cells were maintained in Dulbecco's modified Eagle's medium supplemented with 10% fetal bovine serum at 37 °C under a 5% CO_2 atmosphere. Experiments utilized cells between passages 1 and 10.

Gene knockdown by siRNA and cell treatments

BMVECs were transfected with either SIRT1-specific siRNA (siB14212112732-1-5) or a negative-control siRNA (SiN0000001-1-5) at 50 nM using Lipofectamine RNAiMAX. To evaluate the angiogenic influence of CSS, cells were treated with medium containing 5% CSS-containing rat serum or 5% control serum. For pathway validation, SIRT1-siRNA transfection was combined with CSS-containing serum administration.

CCK8 proliferation assay

Cell viability was determined using the CCK8 assay (CK04-500T, DongRen). Following 2 h incubation with CCK8 reagent, absorbance at 450 nm was measured using a microplate reader. Cell viability was calculated as: (optical density of treated cells / optical density of control cells) × 100%.

Scratch assay

To evaluate lateral cell movement, BMVECs were seeded into six-well plates at 1×10^6 cells per well. Once a uniform monolayer was established, a linear wound was generated using a sterile pipette tip. Images of the scratch region were captured at baseline and following 12 hours of incubation using an inverted microscope (Leica, Germany). Migration capacity was quantified in ImageJ by calculating the relative closure distance, defined as the initial wound width minus the width remaining after 12 hours.

Tube formation assay

For assessing angiogenic capability, 2×10^5 cells per well were plated onto 48-well plates pre-coated with 150 μL of growth factor-reduced Matrigel (352428, Corning, NY, USA). After 12 hours, the formation of capillary-like tubular structures was visualized with an inverted microscope, and quantitative morphometric analysis was performed using ImageJ.

Nuclear and cytoplasmic protein extraction

Subcellular proteins were obtained using a commercial Nuclear and Cytoplasmic Protein Extraction Kit (P0028, Beyotime, Shanghai, China). Cells were first resuspended in solution A and lysed on ice for 15 minutes, followed by addition of solution B and further homogenization. After centrifugation at 13,000 rpm for 5 minutes at 4 °C, the supernatant was collected as the cytoplasmic fraction. The pellet was then processed with solution C, homogenized on ice, and centrifuged at 13,000 rpm for 10 minutes, yielding the nuclear protein fraction.

Enzyme-linked immunosorbent assay

Conditioned media from BMVECs exposed to SIRT1 siRNA, with or without CSS-containing serum, were collected for analysis. VEGFA and BDNF concentrations were measured using ELISA kits (CSB-E04505m; CSB-E04756m, CUSABIO, Wuhan, China) according to manufacturer protocols.

Statistical analysis

All statistical procedures were conducted using SPSS 22.0. Data are expressed as mean ± standard deviation. Group comparisons were examined using one-way ANOVA followed by Tukey's post-hoc test, with $p < 0.05$ considered indicative of significance.

Results and Discussion

Quality assessment of CSS and CSS-containing serum

Multiple hallmark constituents of CSS—including paeoniflorin, liquiritin, ferulic acid, naringin, hesperidin, neohesperidin, glycyrrhizic acid ammonium salt, saikosaponin A, nobiletin, saikosaponin D, tangeretin, and α-cyperone—were successfully identified. Their quantified concentrations complied with the 2020 Chinese Pharmacopeia quality specifications.

CSS alleviated depressive-like phenotypes in CUMS mice

The overall workflow of the experiment is illustrated in **Figure 1a**. Administration of CSS at 19.5 g herb/kg/day produced a marked behavioral improvement in CUMS-exposed mice. As shown in **Figure 1b** and 1C, CUMS animals displayed prominent reductions in both body weight and sucrose preference, consistent with well-recognized depressive manifestations [37]. CSS treatment effectively corrected these deficits, restoring both parameters to near-control levels. Additionally, CUMS mice demonstrated significantly prolonged immobility time in both the TST and FST ($p < 0.01$; $p < 0.01$), whereas CSS administration led to substantial reductions in immobility ($p < 0.05$; $p < 0.01$); **(Figures 1d and 1e)**. Collectively, these observations confirm that CSS exerts pronounced antidepressant-like effects in the CUMS model.

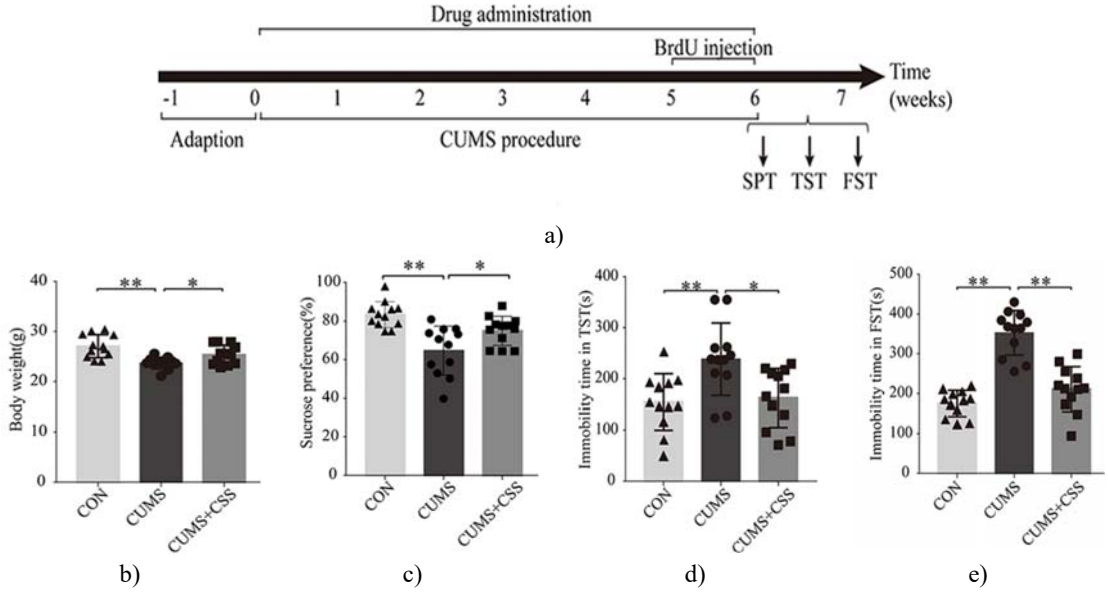

Figure 1. CSS improved depressive behaviors in CUMS mice. (a) Experimental schedule for the study. (b–e) Behavioral outcomes are used to verify the antidepressant actions of CSS. Measurements included body weight (B), the sucrose preference test (c), the tail suspension test (TST) (d), and the forced swim test (FST) (E) across the three experimental groups. Data are presented as mean ± SEM (n = 12). Asterisks denote significance (*$p < 0.05$, **$p < 0.01$).

Hippocampal angiogenesis is involved in the antidepressant effects of CSS

To clarify how CSS mediates its antidepressant properties, network pharmacology analysis was conducted. As illustrated in **Figure 2a**, 147 overlapping therapeutic targets were identified between CSS and MDD. Enrichment analysis demonstrated that these targets were strongly linked to angiogenesis-related pathways. Key enriched biological themes included angiogenesis, endothelial proliferation, vasoconstriction, VEGF regulation, cell

migration, and vascular sprouting, with angiogenesis emerging as the most prominent biological process associated with CSS intervention **(Figure 2b)**.

To experimentally validate these predictions, double immunofluorescence staining for BrdU (a marker of newly generated cells) and GLUT1 (a vascular endothelial marker) was performed to assess angiogenic activity in the hippocampus. Chronic stress markedly reduced the formation of newborn endothelial cells in CUMS mice, reflected by a significant decline in $GLUT1^{+}/BrdU^{+}$ cells compared with the CON group ($p < 0.01$). In contrast, CSS treatment restored endothelial cell generation, leading to a substantial increase in $GLUT1^{+}/BrdU^{+}$ cells ($p < 0.05$), **(Figures 2c and 2d)**, thereby counteracting the CUMS-induced suppression of angiogenesis.

A parallel trend was observed for $CD34^{+}/BrdU^{+}$ cells—another indicator of newly formed vascular endothelial cells. CUMS exposure reduced $CD34^{+}/BrdU^{+}$ cell counts, whereas CSS partially reversed this deficit. Consistent with these findings, the overall number of $BrdU^{+}$ cells was significantly higher in both the CON and CSS-treated groups compared with untreated CUMS mice ($p < 0.01$, $p < 0.05$); **(Figures 2c and 2e).**

Collectively, these observations demonstrate that enhanced hippocampal angiogenesis contributes to the antidepressant effects of CSS.

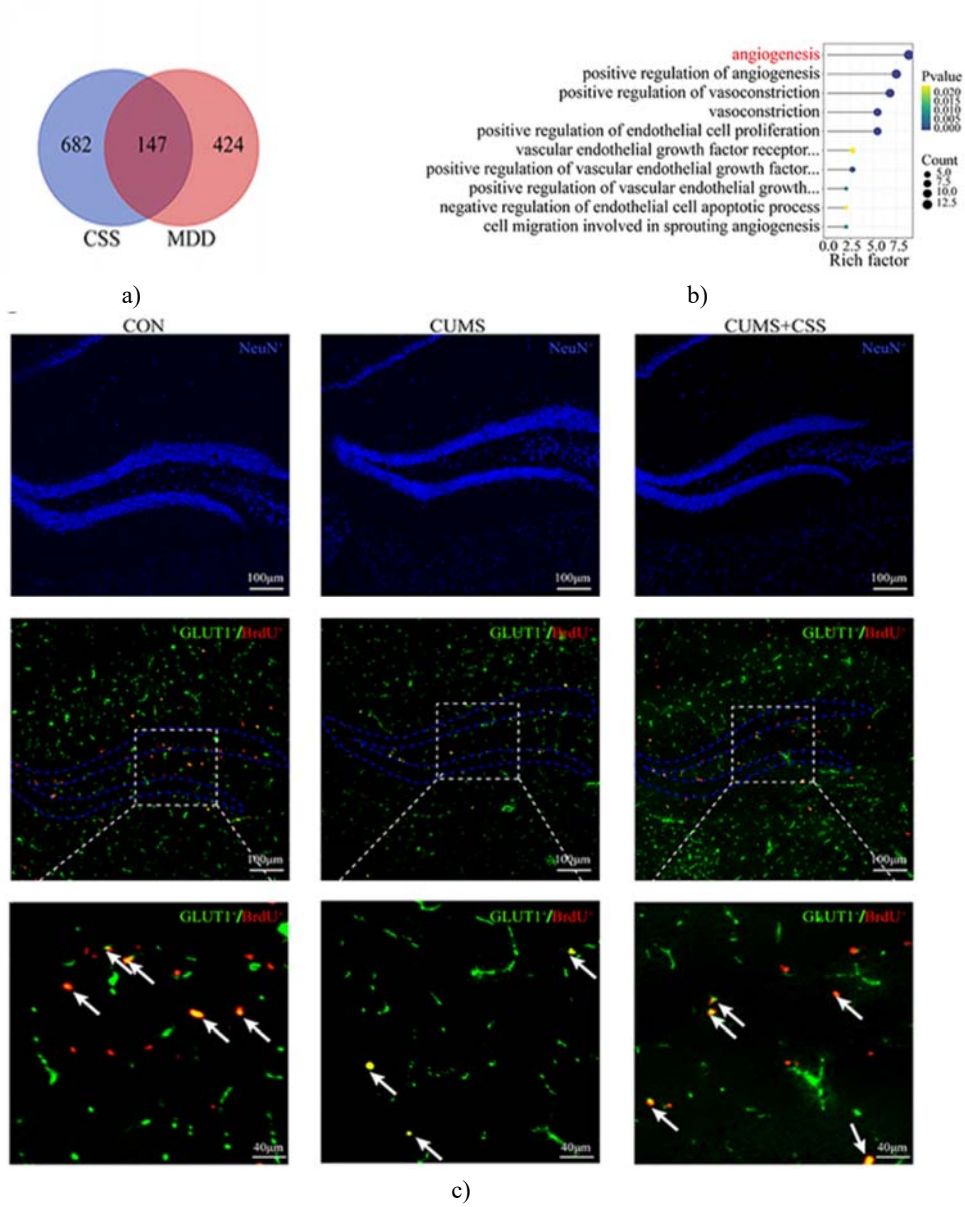

d) e)

Figure 2. The antidepressive actions of CSS were tightly linked to angiogenic mechanisms. (a) Network pharmacology identified 147 shared therapeutic targets between CSS and MDD. (b) Analysis of biological processes associated with these targets highlighted multiple angiogenesis-related pathways. Bubble size reflects the number of genes mapped to each term, while color denotes statistical significance. The Y-axis lists functional annotations, and the X-axis shows the richness factor (number of differentially expressed genes within the pathway divided by the total number of genes in the background set). (c) Confocal imaging revealed the spatial distribution and abundance of $GLUT1^+/BrdU^+$ cells in the hippocampus. BrdU (red) marks newly generated cells, whereas GLUT1 (green) identifies vascular endothelial cells; double-positive cells (indicated by white arrows) represent newborn endothelial cells. (d–e) Quantitative analysis demonstrated changes in $GLUT1^+/BrdU^+$ cell numbers (d) and overall $BrdU^+$ cells (e) in response to CSS. Data are presented as mean ± SEM (n = 3), with significance indicated by *p < 0.05 and **p < 0.01.

SIRT1/FOXO1 axis-mediated hippocampal angiogenesis is involved in the antidepressant effects of CSS in CUMS mice

Further investigation of the central genes regulating angiogenesis through network pharmacology revealed SIRT1 and FOXO1 as major nodes within the protein–protein interaction network, indicating their dominant influence in this regulatory map **(Figures 3a)**. In CUMS mice, hippocampal SIRT1 levels were markedly reduced; however, CSS administration restored SIRT1 expression to significantly higher levels than those observed in untreated CUMS animals ($p < 0.05$, $p < 0.01$); **(Figures 3b and 3c)**.

Conversely, both FOXO1 and acetylated FOXO1 proteins were elevated in CUMS animals when compared with the CON group ($p < 0.05$). CSS exposure normalized these elevations, lowering FOXO1-related protein levels toward those seen in healthy controls ($p < 0.05$); **(Figures 3b, 3d, and 3e)**. Immunohistochemical staining corroborated these findings: as illustrated in **Figure 3f**, CUMS conditions diminished SIRT1 and GLUT1 expression, while simultaneously upregulating FOXO1 within the hippocampus. CSS treatment attenuated these stress-induced alterations.

Importantly, both SIRT1 and FOXO1 were partially localized within hippocampal endothelial cells, supporting the notion that CSS influences endothelial signaling. The observed protein patterns suggest that CSS may enhance FOXO1 cytoplasmic translocation, facilitating its protein degradation and contributing to improved angiogenic activity.

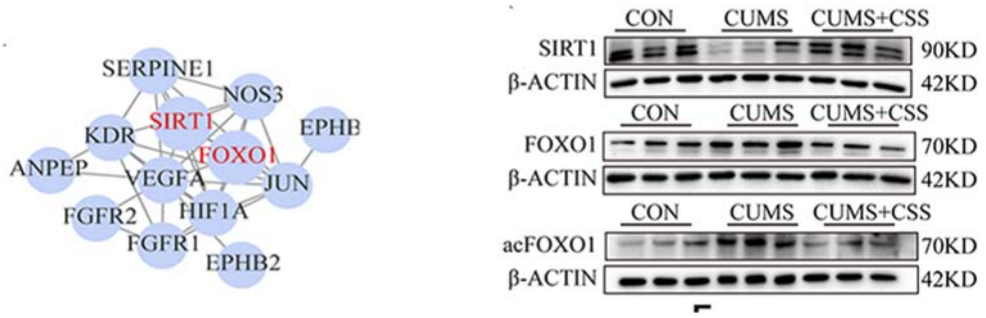

a) b)

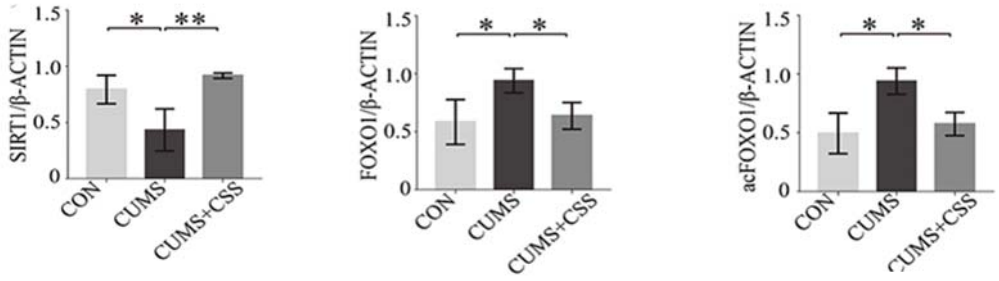

c) d) e)

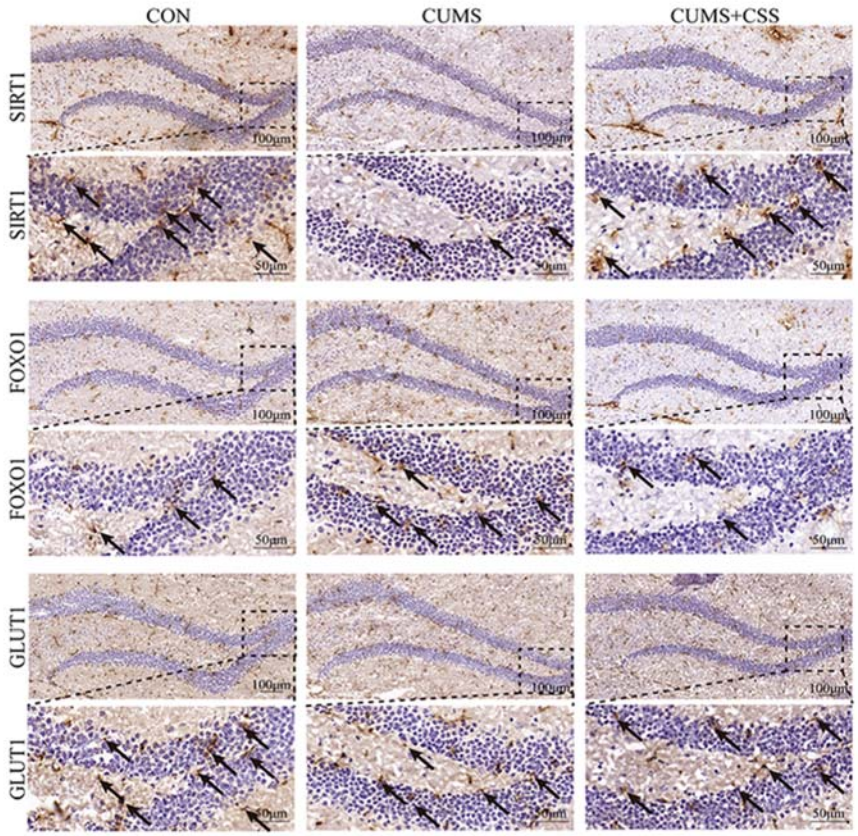

f)

Figure 3. The SIRT1/FOXO1 axis mediates angiogenesis and contributes to the antidepressant effects of CSS.(a) Protein–protein interaction (PPI) network of angiogenesis-related targets, where nodes indicate targets and lines represent interactions between them.(b) Representative Western blot images illustrating the influence of CSS on the SIRT1/FOXO1 axis in CUMS mice, with or without CSS treatment. Quantification of (c) SIRT1, (d) total FOXO1, and (e) acetylated FOXO1 (ac-FOXO1) levels, using β-ACTIN as the internal control.(f) Immunohistochemical detection of SIRT1, FOXO1, and GLUT1 proteins in the hippocampus across the three groups (magnifications ×200 and ×600). Black arrows indicate positive staining. Data are expressed as mean ± SEM (n = 3); *p < 0.05, **p < 0.01 denote significant differences.

CSS-containing serum promotes BMVECs proliferation, migration, and tube formation via SIRT1

CCK8 assays revealed that treating BMVECs with 5% CSS-containing serum for 12 h produced the maximal proliferative response in both a dose- and time-dependent manner **(Figures 4a and 4b)**. Accordingly, 5% CSS serum was selected for all subsequent in vitro experiments. To determine the role of SIRT1 in CSS-mediated angiogenesis, target-specific siRNA knockdown was applied in BMVECs.

As shown in **Figures 4c and 4d**, CSS serum significantly increased BMVEC proliferation at 6 h and 12 h, whereas SIRT1 silencing (si-SIRT1 + CSS) markedly attenuated this effect ($p < 0.01$). Similarly, cell migration was significantly enhanced after 12 h of CSS serum exposure compared with the control serum ($p < 0.01$), but SIRT1 knockdown effectively abolished this enhancement ($p < 0.01$); **(Figures 4e and 4f)**.

Tube formation assays further confirmed the proangiogenic role of CSS. Treatment with 5% CSS serum significantly increased mesh formation and branching lengths ($p < 0.05$) and modestly elevated node numbers, while these effects were neutralized by SIRT1-specific siRNA **(Figures 4g–4j)**.

Collectively, these findings demonstrate that CSS promotes BMVEC angiogenesis primarily through SIRT1-dependent mechanisms.

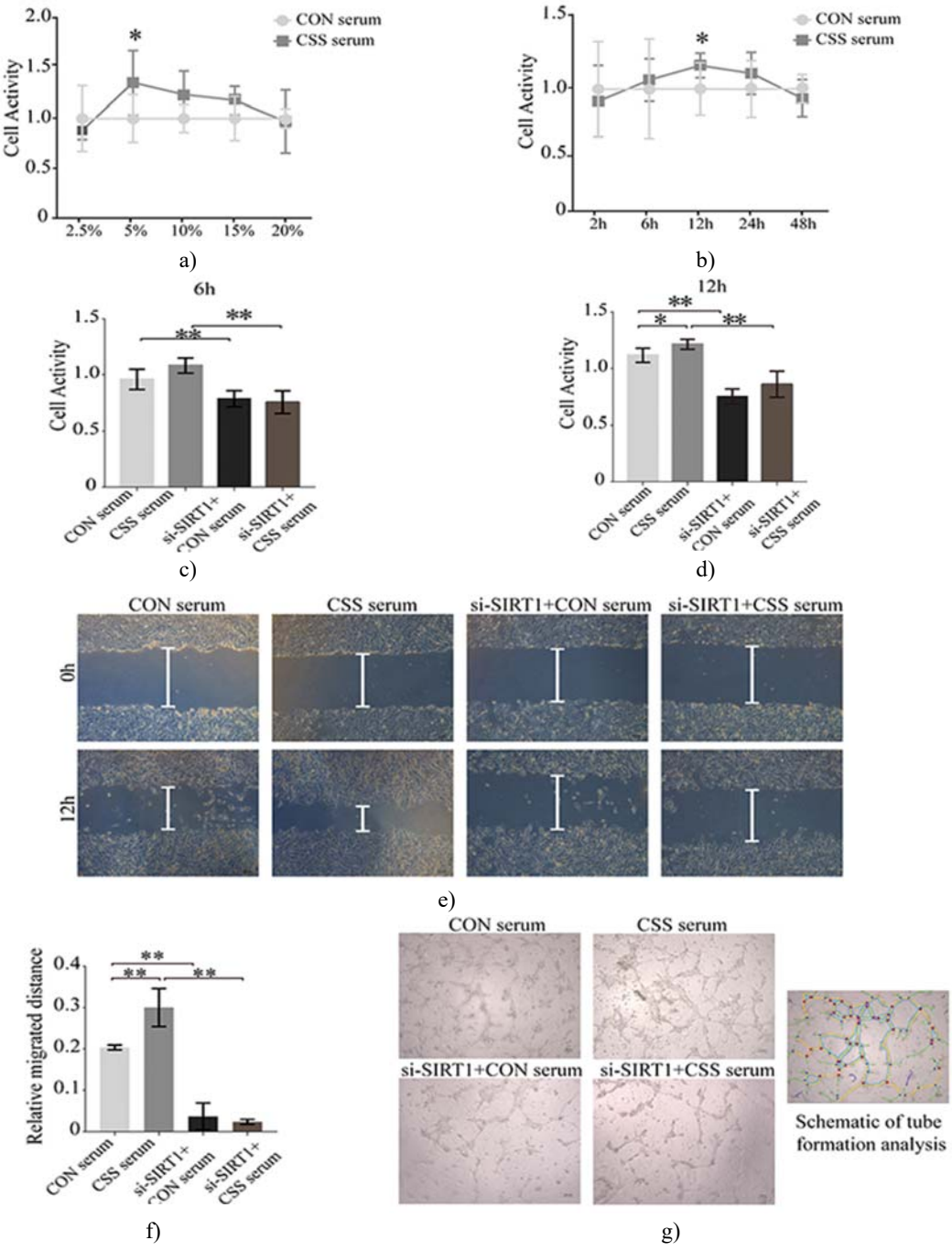

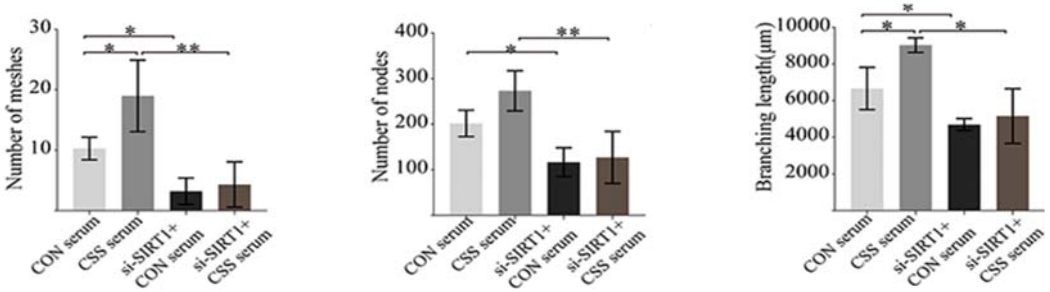

h) i) j)

Figure 4. CSS enhances endothelial cell angiogenic functions via SIRT1. (a) Proliferation of BMVECs in response to varying concentrations of CSS-containing serum (2.5–20%) at 12 h.(b) Time-course proliferation of BMVECs treated with 5% CSS serum at 2, 6, 12, 24, and 48 h.(c, d) Effects of SIRT1 on CSS-induced proliferation at 6 h and 12 h. (e) Representative images of BMVEC migration at 12 h (n = 6). (f) Quantitative analysis of migration distances measured by scratch assay. (g) Representative tube formation images at 12 h, with blue circles indicating meshes, pink and yellow dots representing nodes, and lines showing branches. (h–j) Quantification of mesh numbers (h), nodes (i), and branching lengths (j) in the tube formation assay. Data are shown as mean ± SEM (n = 3); *p < 0.05, **p < 0.01.

FOXO1 acts as a downstream effector of SIRT1 in CSS-induced angiogenesis

To further explore downstream mediators of SIRT1, we examined FOXO1 in BMVECs. As depicted in **Figures 5a–5d**, inhibition of SIRT1 increased both total and acetylated FOXO1 levels, regardless of CSS serum treatment ($p < 0.01$).

Subcellular localization of FOXO1 was assessed to evaluate its activation state **(Figures 5e–5g)**. In the CSS serum group, cytoplasmic FOXO1 levels were elevated compared with control serum, whereas SIRT1 knockdown reversed this effect ($p < 0.05$). Conversely, nuclear FOXO1 was reduced in the CSS serum group compared with control, but this reduction was significantly counteracted by SIRT1 silencing ($p < 0.01$). Notably, nuclear FOXO1 is transcriptionally active and inhibits angiogenesis.

Immunofluorescence further confirmed these findings **(Figure 5h)**, showing that SIRT1 predominantly localized in the nucleus, while FOXO1 shifted to the cytoplasm after CSS serum treatment. This cytoplasmic relocation of FOXO1 was abolished in siRNA-SIRT1-transfected cells, consistent with the Western blot results.

Overall, these data indicate that the pro-angiogenic effects of CSS in BMVECs are mediated through the SIRT1/FOXO1 signaling axis.

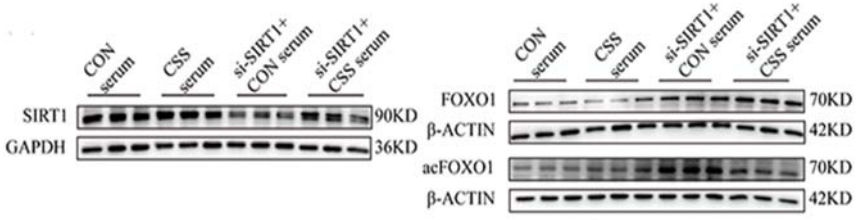

a)

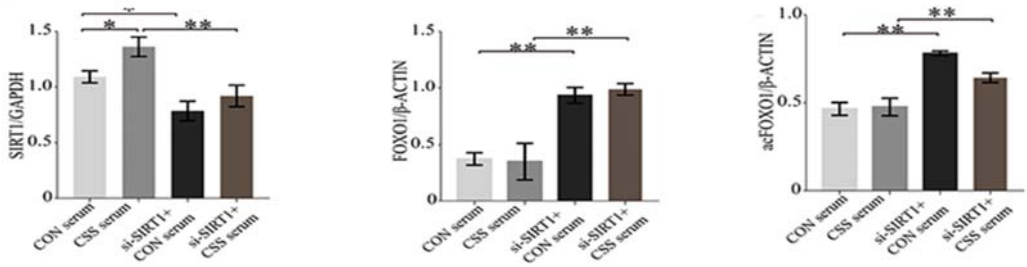

c) d) e)

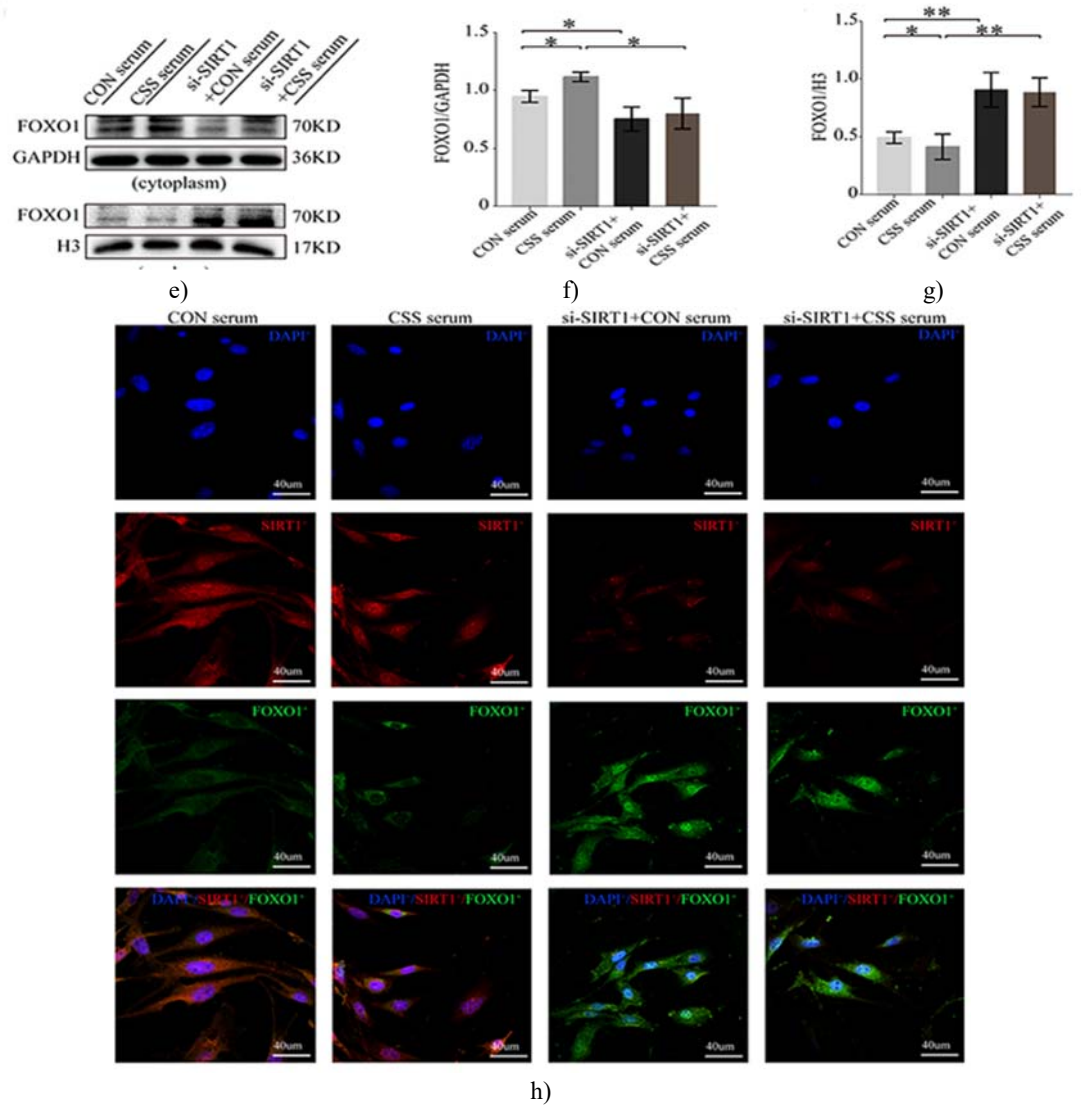

Figure 5. FOXO1, as a downstream effector of SIRT1, contributes to the pro-angiogenic activity of CSS-containing serum. (a) Western blot analysis of SIRT1, FOXO1, and acetylated FOXO1 (acFOXO1) protein levels in BMVECs. Quantitative results of SIRT1 (b), FOXO1 (c), and acFOXO1 (d) are shown. (e) Western blots of cytoplasmic and nuclear FOXO1. Quantification of cytosolic FOXO1 (f) and nuclear FOXO1 (g). (h) Representative immunofluorescence images of BMVECs (×600) showing SIRT1 in red and FOXO1 in green; nuclei are stained with DAPI (blue). Data are expressed as mean ± SEM (n = 3); *p < 0.05, **p < 0.01.

CSS Enhances neurotrophic Factor expression and secretion, potentially supporting neurogenesis

As illustrated in **Figures 6a–6c**, BDNF and VEGFA protein levels were markedly reduced in the hippocampus of CUMS mice but were significantly restored following CSS treatment ($p < 0.05$). To examine the role of SIRT1 in this process, we assessed neurotrophic factor expression and secretion in BMVECs. Western blot analysis (**Figures 6d–6f)** demonstrated that SIRT1 knockdown decreased BDNF and VEGFA levels even in the presence of CSS-containing serum.

Furthermore, enzyme-linked immunosorbent assay showed that CSS serum treatment significantly increased BDNF and VEGFA secretion into the culture medium compared with control serum ($p < 0.05$). This effect was abolished in SIRT1-deficient BMVECs ($p < 0.01$, $p < 0.05$); **(Figures 6g–6h)**.

In addition, analysis of hippocampal neurogenesis revealed that NeuN+/BrdU+ and GLUT1+/BrdU+ cell populations were significantly reduced in CUMS mice, but CSS treatment effectively prevented these decreases.

Collectively, these findings suggest that CSS or CSS-containing serum promotes neurotrophic factor expression and secretion in both the hippocampus of CUMS mice and BMVECs, which may facilitate neurogenesis.

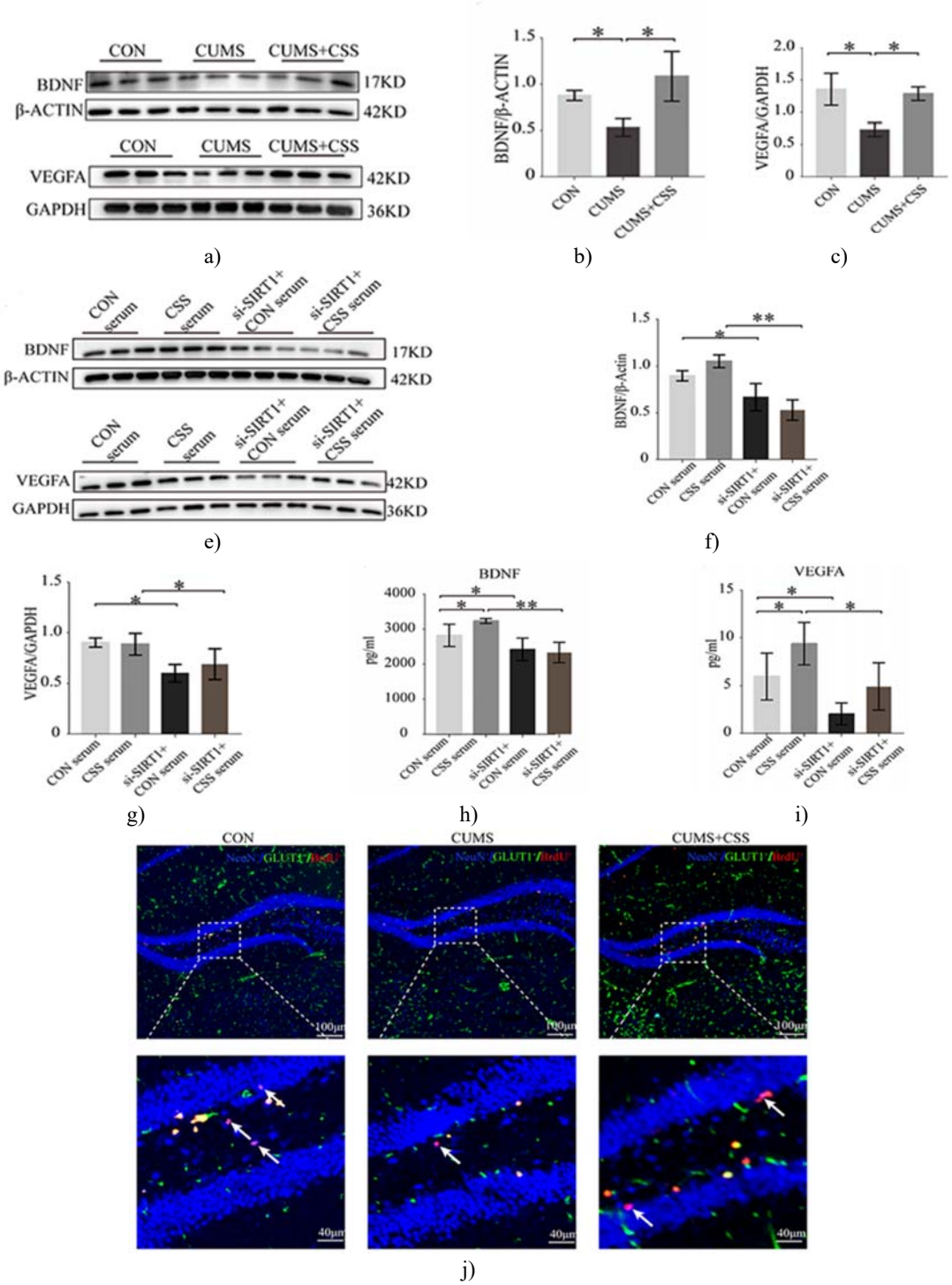

Figure 6. CSS stimulated the production and release of neurotrophic factors, which may promote neurogenesis. In the hippocampus, BDNF and VEGFA levels were examined via Western blotting (a), followed by quantitative assessment of BDNF (b) and VEGFA (c) protein levels. Similarly, in BMVECs, Western blotting was performed to detect BDNF and VEGFA expression, with corresponding quantitative analyses for BDNF (e) and VEGFA (f) proteins (D). The concentrations of BDNF and VEGFA in the culture medium were determined using ELISA (g, h; n=5). Confocal microscopy (i) revealed the localization and

quantity of newly formed cells in the hippocampus, with newborn endothelial cells labeled as GLUT1+/BrdU+ (green/red) and newly generated neurons as NeuN+/BrdU+ (blue/red); white arrows indicate newborn neurons (n=3). Asterisks denote statistically significant differences (*$p < 0.05$; **$p < 0.01$).

Chaihu Shugan San (CSS) is a traditional Chinese medicine (TCM) commonly applied in the clinical management of major depressive disorder (MDD) in China. Previous research has indicated that CSS exerts antidepressant effects through multiple biological pathways, including anti-inflammatory activity, regulation of the hypothalamic-pituitary-adrenal axis, inhibition of neurotransmitter reuptake, and promotion of neurogenesis [38–40]. Nonetheless, due to the complex mixture of bioactive compounds in CSS, its precise mechanisms remain insufficiently understood, necessitating further investigation to broaden its therapeutic use in MDD. Our current study provides compelling evidence supporting CSS as an effective treatment for MDD. Behavioral assessments revealed that CSS alleviated anhedonia and despair in chronic unpredictable mild stress (CUMS) mice, consistent with earlier findings [41, 42].

High-performance liquid chromatography/mass spectrometry identified key constituents of CSS, including Saikosaponin A from Bupleurum falcatum L., naringin, hesperidin, and neohesperidin from Citrus reticulata Blanco and Citrus × aurantium L., paeoniflorin from Paeonia lactiflora Pall., ferulic acid from Ligusticum chuanxiong Hort., and liquiritin and glycyrrhizic acid ammonium salt from Glycyrrhiza uralensis Fisch. These findings are valuable for quality control of CSS and may help clarify the roles of individual compounds.

Network pharmacology analysis, which constructs a “compound–protein/gene–disease” network, is effective in uncovering the complex interactions among diseases, therapeutic targets, and multiple TCM compounds [43]. Our results suggested that CSS-mediated antidepressant effects were closely linked to angiogenesis. Previous studies have shown that both depressed patients and animal models exhibit dysregulated expression of angiogenic genes or proteins, such as VEGFR2 and endoglin [44–46]. Transcriptomic analysis of dentate gyrus cells from postmortem MDD brains also demonstrated upregulation of anti-angiogenic genes [47]. Clinically, enhanced angiogenesis has been associated with improved responses to antidepressant therapy, and electroconvulsive seizure treatment has been reported to strongly induce hippocampal angiogenesis [48]. VEGFA, a key pro-angiogenic factor, has been shown to mimic antidepressant effects and potentially augment responses to conventional treatments [49]. Conversely, clinical trials using angiogenesis inhibitors like interferon-α and belimumab reported an increased incidence of depressive symptoms [50, 51]. In our study, CSS treatment increased the formation of new microvessels in the hippocampus of CUMS mice, providing direct evidence that CSS promotes angiogenesis. These findings suggest that targeting angiogenic pathways may offer a promising strategy for enhancing antidepressant therapy.

Angiogenesis is regulated by multiple signaling cascades, among which SIRT1 plays a critical role by deacetylating FOXO1 and thereby counteracting FOXO1-mediated inhibition of angiogenesis. Activation of SIRT1 has been shown to enhance angiogenesis and improve conditions such as cerebral ischemic injury [52], diabetic wound healing [24], and arthritis [53]. Our network pharmacology analysis highlighted SIRT1 and FOXO1 as central nodes in the protein–protein interaction network, indicating that this pathway is pivotal for the antidepressant effects of CSS. Experiments revealed that SIRT1 and FOXO1 were predominantly expressed in vascular endothelial cells, and CSS treatment upregulated SIRT1 while downregulating FOXO1 and acetylated FOXO1 (acFOXO1). Using SIRT1 siRNA to reverse these effects partially confirmed that CSS promotes angiogenesis through the SIRT1/FOXO1 axis. Moreover, SIRT1 regulates FOXO1 nuclear-cytoplasmic shuttling in response to various stimuli [54, 55]. In endothelial cells, nuclear FOXO1 exhibits strong transcriptional activity, regulating downstream targets such as VEGFA, c-MYC, and CD36, which inhibit angiogenesis [56–58]. Our findings showed that CSS serum facilitated FOXO1 translocation from the nucleus to the cytoplasm, reducing its activity and thereby promoting angiogenesis. This suggests that SIRT1 upregulation is a key mechanism by which CSS enhances angiogenic activity. Pharmacologic or genetic ablation of hippocampal SIRT1 has been associated with increased depressive behaviors in mice [59], whereas SIRT1 activators such as resveratrol exhibit antidepressant-like effects [60]. Therefore, targeting SIRT1 may provide a valuable approach for developing natural compound-based therapies for MDD.

Neurogenesis is closely intertwined with angiogenesis, as neural stem cells reside in neurovascular niches where endothelial cells provide direct contacts and secrete neurotrophic factors such as VEGFA and BDNF [61]. Previous studies have demonstrated that elevated VEGFA and/or BDNF levels enhance hippocampal neurogenesis and ameliorate depressive behaviors [20]. Consistent with these findings, our results showed that

CSS increased VEGFA and BDNF expression in the hippocampus of depressive mice and in BMVEC supernatants, indicating that CSS promotes both expression and secretion of neurotrophic factors to support neurogenesis. This coordinated promotion of angiogenesis and neurogenesis likely contributes to the antidepressant effects of CSS, potentially via the SIRT1/FOXO1 axis. However, these findings are preliminary, and further studies are necessary to elucidate the detailed molecular mechanisms underlying CSS-mediated angiogenesis and neurogenesis in CUMS mice.

Conclusion

This study demonstrates that CSS alleviates depressive-like behaviors in CUMS mice, potentially through enhanced angiogenesis mediated by the SIRT1/FOXO1 pathway. In vitro, CSS promoted BMVEC proliferation, migration, and tube formation, as well as the expression and secretion of neurotrophic factors, effects that were attenuated by SIRT1 silencing. These results provide novel insights into the clinical potential of CSS and deepen our understanding of its mechanisms in depression.

Acknowledgments: None

Conflict of Interest: None

Financial Support: None

Ethics Statement: None

References

1. Malhi GS, Mann JJ. Depression. Lancet. 2018;392(10161):2299-312. doi:10.1016/S0140-6736(18)31948-2
2. Cleare A, Pariante CM, Young AH, Anderson IM, Christmas D, Cowen PJ, et al. Evidence-based guidelines for treating depressive disorders with antidepressants: a revision of the 2008 British Association for Psychopharmacology guidelines. J Psychopharmacol. 2015;29(5):459-525. doi:10.1177/0269881115581093
3. Serretti A, Mandelli L, Raffaella P, Enrico S, Alberto C. Gastrointestinal side effects associated with antidepressant treatments in patients with major depressive disorder: a systematic review and meta-analysis. Prog Neuropsychopharmacol Biol Psychiatry. 2021;109:110266. doi:10.1016/j.pnpbp.2021.110266
4. Serretti A, Chiesa A. Treatment-emergent sexual dysfunction related to antidepressants: a meta-analysis. J Clin Psychopharmacol. 2009;29(3):259-66. doi:10.1097/JCP.0b013e3181a5233f
5. Ballard ED, Zarate CA Jr. The role of dissociation in ketamine's antidepressant effects. Nat Commun. 2020;11(1):6431. doi:10.1038/s41467-020-20190-4
6. Newport DJ, Schatzberg AF, Nemeroff CB. Whither ketamine as an antidepressant: panacea or toxin? Depress Anxiety. 2016;33(8):685-8. doi:10.1002/da.22535
7. Milev RV, Giacobbe P, Kennedy SH, Blumberger DM, Daskalakis ZJ, Downar J, et al. Canadian Network for Mood and Anxiety Treatments (CANMAT) 2016 clinical guidelines for the management of adults with major depressive disorder: section 4. Neurostimulation treatments. Can J Psychiatry. 2016;61(9):561-75. doi:10.1177/0706743716660033
8. Cuijpers P, Quero S, Dowrick C, Arroll B. Psychological treatment of depression in primary care: recent developments. Curr Psychiatry Rep. 2019;21(12):129. doi:10.1007/s11920-019-1117-x
9. Jin WD, Xing BP, Wang HQ, Chen J. Meta-analysis of clinical efficacy of Chaihu Shugansan in treatment of depression. Zhongguo Zhong Yao Za Zhi. 2009;27(7):1397-9. Chinese. doi:10.13193/j.archtcm.2009.07.54.jinwd.024
10. Yeung WF, Chung KF, Ng KY, Yu YM, Ziea ET, Ng BF. A systematic review on the efficacy, safety and types of Chinese herbal medicine for depression. J Psychiatr Res. 2014;57:165-75. doi:10.1016/j.jpsychires.2014.05.016

11. Wang Y, Fan R, Huang X. Meta-analysis of the clinical effectiveness of traditional Chinese medicine formula Chaihu-Shugan-San in depression. J Ethnopharmacol. 2012;141(2):571-7. doi:10.1016/j.jep.2011.08.079
12. Chen XQ, Li CF, Chen SJ, Liang W, Wang Y, Li ZW, et al. The antidepressant-like effects of Chaihu Shugan San: dependent on the hippocampal BDNF-TrkB-ERK/Akt signaling activation in perimenopausal depression-like rats. Biomed Pharmacother. 2018;105:45-52. doi:10.1016/j.biopha.2018.04.035
13. Yan L, Xu X, He Z, Wang S, Zhao L, Qiu J, et al. Antidepressant-like effects and cognitive enhancement of coadministration of Chaihu Shugan San and fluoxetine: dependent on the BDNF-ERK-CREB signaling pathway in the hippocampus and frontal cortex. Biomed Res Int. 2020;2020:2794263. doi:10.1155/2020/2794263
14. Li L, Yu AL, Wang ZL, Wang YL, Chen L, Zhang HQ. Chaihu-Shugan-San and absorbed meranzin hydrate induce anti-atherosclerosis and behavioral improvements in high-fat diet ApoE(-/-) mice via anti-inflammatory and BDNF-TrkB pathway. Biomed Pharmacother. 2019;115:108893. doi:10.1016/j.biopha.2019.108893
15. Qiu J, Hu SY, Shi GQ, Wang SE. Changes in regional cerebral blood flow with Chaihu-Shugan-San in the treatment of major depression. Pharmacogn Mag. 2014;10(40):503-8. doi:10.4103/0973-1296.141775
16. Yamada MK. Angiogenesis in refractory depression: a possible phenotypic target to avoid the blood brain barrier. Drug Discov Ther. 2016;10(2):74-8. doi:10.5582/ddt.2016.01003
17. Almeida OP, Ford AH, Flicker L, Hankey GJ, Yeap BB, Golledge J, et al. Angiogenesis inhibition and depression in older men. J Psychiatry Neurosci. 2014;39(3):200-5. doi:10.1503/jpn.130158
18. Boldrini M, Hen R, Underwood MD, Rosoklija GB, Dwork AJ, Mann JJ, et al. Hippocampal angiogenesis and progenitor cell proliferation are increased with antidepressant use in major depression. Biol Psychiatry. 2012;72(7):562-71. doi:10.1016/j.biopsych.2012.04.024
19. Duman RS, Deyama S, Fogaça MV. Role of BDNF in the pathophysiology and treatment of depression: activity-dependent effects distinguish rapid-acting antidepressants. Eur J Neurosci. 2021;53(1):126-39. doi:10.1111/ejn.14630
20. Khan A, Shal B, Naveed M, Nasir B, Khan NU, Ullah I, et al. Matrine ameliorates anxiety and depression-like behaviour by targeting hyperammonemia-induced neuroinflammation and oxidative stress in CCl4 model of liver injury. Neurotoxicology. 2019;72:38-50. doi:10.1016/j.neuro.2019.02.002
21. Shi Y, Luan D, Song R, Zhang Z. Value of peripheral neurotrophin levels for the diagnosis of depression and response to treatment: a systematic review and meta-analysis. Eur Neuropsychopharmacol. 2020;41:40-51. doi:10.1016/j.euroneuro.2020.09.633
22. Kiuchi T, Lee H, Mikami T. Regular exercise cures depression-like behavior via VEGF-Flk-1 signaling in chronically stressed mice. Neuroscience. 2012;207:208-17. doi:10.1016/j.neuroscience.2012.01.023
23. Li X, Wu G, Han F, Wang Z, Liu X, Wang Q, et al. SIRT1 activation promotes angiogenesis in diabetic wounds by protecting endothelial cells against oxidative stress. Arch Biochem Biophys. 2019;661:117-24. doi:10.1016/j.abb.2018.11.016
24. Huang X, Sun J, Chen G, Niu C, Wang Y, Zhao C, et al. Resveratrol promotes diabetic wound healing via SIRT1-FOXO1-c-Myc signaling pathway-mediated angiogenesis. Front Pharmacol. 2019;10:421. doi:10.3389/fphar.2019.00421
25. Liu W, Yan H, Zhou D, Cai X, Dong Y, Li C, et al. The depression GWAS risk allele predicts smaller cerebellar gray matter volume and reduced SIRT1 mRNA expression in Chinese population. Transl Psychiatry. 2019;9(1):333. doi:10.1038/s41398-019-0675-3
26. Ning HE, Ling JH, Liang G, Zhang Z, Wang YJ. Effects of Chaihu Shugan powder on the cytoactivity of rat interstitial cells of Cajal and intracellular Ca2+ concentration. Zhongguo Zhong Xi Yi Jie He Za Zhi. 2016;36(9):1091-6. Chinese.
27. Zhang S, Lu Y, Chen W, Shi W, Zhao W, Liu L, et al. Network pharmacology and experimental evidence: PI3K/AKT signaling pathway is involved in the antidepressive roles of Chaihu Shugan San. Drug Des Devel Ther. 2021;15:3425-41. doi:10.2147/DDDT.S315060
28. Liu MY, Yin CY, Zhu LJ, Zhu XH, Xu C, Luo CX, et al. Sucrose preference test for measurement of stress-induced anhedonia in mice. Nat Protoc. 2018;13(7):1686-98. doi:10.1038/s41596-018-0011-z

29. Nishino T, Tamada K, Maeda A, Abe H, Ito H, Imai Y, et al. Behavioral analysis in mice deficient for GAREM2 (Grb2-associated regulator of Erk/MAPK subtype2) that is a subtype of highly expressing in the brain. Mol Brain. 2019;12(1):94. doi:10.1186/s13041-019-0512-x
30. Cryan JF, Mombereau C, Vassout A. The tail suspension test as a model for assessing antidepressant activity: review of pharmacological and genetic studies in mice. Neurosci Biobehav Rev. 2005;29(4-5):571-625. doi:10.1016/j.neubiorev.2005.03.009
31. Le-Niculescu H, Case NJ, Hulvershorn L, Patel SD, Bowker J, Gupta J, et al. Convergent functional genomic studies of ω-3 fatty acids in stress reactivity, bipolar disorder and alcoholism. Transl Psychiatry. 2011;1(4):e4. doi:10.1038/tp.2011.1
32. Qu M, Zhao J, Zhao Y, Zhang J, Yuan Y, Feng Y, et al. Vascular protection and regenerative effects of intranasal DL-3-N-butylphthalide treatment after ischaemic stroke in mice. Stroke Vasc Neurol. 2021;6(1):74-9. doi:10.1136/svn-2020-000364
33. McCrary MR, Jiang MQ, Giddens MM, Zhang NY, Lewis KM, Wahl SE, et al. Protective effects of GPR37 via regulation of inflammation and multiple cell death pathways after ischemic stroke in mice. FASEB J. 2019;33(10):10680-91. doi:10.1096/fj.201900070R
34. Yu SP, Tung JK, Wei ZZ, Chen D, Liang J, Constable A, et al. Optochemogenetic stimulation of transplanted iPS-NPCs enhances neuronal repair and functional recovery after ischemic stroke. J Neurosci. 2019;39(33):6571-94. doi:10.1523/JNEUROSCI.2010-18.2019
35. Yan GJ, Zhao HM, Hong X. LncRNA MACC1-AS1 attenuates microvascular endothelial cell injury and promotes angiogenesis under hypoxic conditions via modulating miR-6867-5p/TWIST1 in human brain microvascular endothelial cells. Ann Transl Med. 2021;8(14):876. doi:10.21037/atm-20-4915
36. Zeng W, Lei QL, Ma J, Gao S, Ju Z. Endothelial progenitor cell-derived microvesicles promote angiogenesis in rat brain microvascular endothelial cells in vitro. Front Cell Neurosci. 2021;15:638351. doi:10.3389/fncel.2021.638351
37. Burstein O, Doron R. The unpredictable chronic mild stress protocol for inducing anhedonia in mice. J Vis Exp. 2018;(140):58184. doi:10.3791/58184
38. Han SK, Kim JK, Park HS, Shin YJ, Kim DH. Chaihu-Shugan-San (Shihosogansan) alleviates restraint stress-generated anxiety and depression in mice by regulating NF-κB-mediated BDNF expression through the modulation of gut microbiota. Chin Med. 2021;16(1):77. doi:10.1186/s13020-021-00492-5
39. Liu Q, Sun NN, Wu ZZ, Fan DH, Cao MQ. Chaihu-Shugan-San exerts an antidepressive effect by downregulating miR-124 and releasing inhibition of the MAPK14 and Gria3 signaling pathways. Neural Regen Res. 2018;13(5):837-45. doi:10.4103/1673-5374.232478
40. Li YH, Zhang CH, Wang SE, Qiu J, Hu SY, Xiao GL. Effects of Chaihu Shugan San on behavior and plasma levels of corticotropin releasing hormone and adrenocorticotropic hormone of rats with chronic mild unpredicted stress depression. Zhong Xi Yi Jie He Xue Bao. 2009;7(11):1073-7. Chinese. doi:10.3736/jcim20091110
41. Zhang H, Huang H, Song H, Liu X, Zhang H. Serum metabolomics reveals the intervention mechanism and compatible regularity of Chaihu Shu Gan San on chronic unpredictable mild stress-induced depression rat model. J Pharm Pharmacol. 2020;72(8):1133-43. doi:10.1111/jphp.13286
42. Sun KH, Jin Y, Mei ZG, Sun ZQ. Antidepressant-like effects of Chaihu Shugan powder on rats exposed to chronic unpredictable mild stress through inhibition of endoplasmic reticulum stress-induced apoptosis. Chin J Integr Med. 2021;27(5):353-60. doi:10.1007/s11655-020-3228-y
43. Zhang R, Zhu X, Bai H, Ning K. Network pharmacology databases for traditional Chinese medicine: review and assessment. Front Pharmacol. 2019;10:123. doi:10.3389/fphar.2019.00123
44. Pantazatos SP, Huang YY, Rosoklija GB, Dwork AJ, Arango V, Mann JJ. Whole-transcriptome brain expression and exon-usage profiling in major depression and suicide: evidence for altered glial, endothelial and ATPase activity. Mol Psychiatry. 2017;22(5):760-73. doi:10.1038/mp.2016.130
45. Van Den Bossche MJA, Emsell L, Dols A, Stek ML, Blumberger DM, Poulet E, et al. Hippocampal volume change following ECT is mediated by rs699947 in the promotor region of VEGF. Transl Psychiatry. 2019;9(1):191. doi:10.1038/s41398-019-0530-6
46. Lehmann ML, Poffenberger CN, Elkahloun AG, Herkenham M. Analysis of cerebrovascular dysfunction caused by chronic social defeat in mice. Brain Behav Immun. 2020;88:735-47. doi:10.1016/j.bbi.2020.05.030

47. Mahajan GJ, Vallender EJ, Garrett MR, Challagundla L, Overholser JC, Jurjus G, et al. Altered neuro-inflammatory gene expression in hippocampus in major depressive disorder. Prog Neuropsychopharmacol Biol Psychiatry. 2018;82:177-86. doi:10.1016/j.pnpbp.2017.11.017
48. Nuninga JO, Mandl RCW, Froeling M, Siero JCW, Somers M, Boks MP, et al. Vasogenic edema versus neuroplasticity as neural correlates of hippocampal volume increase following electroconvulsive therapy. Brain Stimul. 2020;13(4):1080-6. doi:10.1016/j.brs.2020.04.017
49. Warner-Schmidt JL, Duman RS. VEGF as a potential target for therapeutic intervention in depression. Curr Opin Pharmacol. 2008;8(1):14-9. doi:10.1016/j.coph.2007.10.013
50. Whale R, Fialho R, Field AP, Rolt M, Eccles J, Fernandes M, et al. Factor analyses differentiate clinical phenotypes of idiopathic and interferon-alpha-induced depression. Brain Behav Immun. 2019;80:519-24. doi:10.1016/j.bbi.2019.04.035
51. Minnema LA, Giezen TJ, Souverein PC, Egberts TCG, Leufkens HGM, Gardarsdottir H. Exploring the association between monoclonal antibodies and depression and suicidal ideation and behavior: a VigiBase study. Drug Saf. 2019;42(7):887-95. doi:10.1007/s40264-018-00789-9
52. Zheng XW, Shan CS, Xu QQ, Wang Y, Shi YH, Wang Y. Buyang Huanwu decoction targets SIRT1/VEGF pathway to promote angiogenesis after cerebral ischemia/reperfusion injury. Front Neurosci. 2018;12:911. doi:10.3389/fnins.2018.00911
53. Leblond A, Pezet S, Cauvet A, Fournier M, Giraud C, Gorwood P, et al. Implication of the deacetylase sirtuin-1 on synovial angiogenesis and persistence of experimental arthritis. Ann Rheum Dis. 2020;79(7):891-900. doi:10.1136/annrheumdis-2020-217377
54. Choi HK, Cho KB, Phuong NT, Han CY, Nam HS, Han CY, et al. SIRT1-mediated FoxO1 deacetylation is essential for multidrug resistance-associated protein 2 expression in tamoxifen-resistant breast cancer cells. Mol Pharm. 2013;10(7):2517-27. doi:10.1021/mp400287p
55. Chen S, Zhao Z, Ke L, Yang J, Zhang L, Liu Y, et al. Resveratrol improves glucose uptake in insulin-resistant adipocytes via Sirt1. J Nutr Biochem. 2018;55:209-18. doi:10.1016/j.jnutbio.2018.02.007
56. Wilhelm K, Happel K, Eelen G, Schoors S, Oellerich MF, Lim R, et al. FOXO1 couples metabolic activity and growth state in the vascular endothelium. Nature. 2016;529(7585):216-20. doi:10.1038/nature16498
57. Jeon HH, Yu Q, Lu Y, Spencer E, Lu C, Zhang Y, et al. FOXO1 regulates VEGFA expression and promotes angiogenesis in healing wounds. J Pathol. 2018;245(3):258-64. doi:10.1002/path.5075
58. Ren B. FoxO1 transcriptional activities in VEGF expression and beyond: a key regulator in functional angiogenesis? J Pathol. 2018;245(3):255-7. doi:10.1002/path.5088
59. Abe-Higuchi N, Uchida S, Yamagata H, Higuchi F, Hobara T, Hara K, et al. Hippocampal sirtuin 1 signaling mediates depression-like behavior. Biol Psychiatry. 2016;80(11):815-26. doi:10.1016/j.biopsych.2016.01.009
60. Moore A, Beidler J, Hong MY. Resveratrol and depression in animal models: a systematic review of the biological mechanisms. Molecules. 2018;23(9):2197. doi:10.3390/molecules23092197
61. Segarra M, Aburto MR, Hefendehl J, Acker-Palmer A. Neurovascular interactions in the nervous system. Annu Rev Cell Dev Biol. 2019;35:615-35. doi:10.1146/annurev-cellbio-100818-125142